Catalysis Science & Technology

Accepted Manuscript

ROYAL SOCIETY OF CHEMISTRY

www.rsc.org/catalysis

Journal Name

ARTICLE

Mechanism and material aspects of novel Ag_2O/TiO_2 photo-catalyst active in infrared radiation for water splitting

Received 00th January 20xx,
Accepted 00th January 20xx

DOI: 10.1039/x0xx00000x

www.rsc.org/

A. Gannoruwa[a], B. Ariyasinghe[a], J. Bandara[a*]

The Ag_2O/TiO_2 catalyst produces hydrogen with water and water/methanol mixture when irradiated with IR light. In this report, material aspects and the photocatalytic mechanism of the IR active photocatalyst Ag_2O/TiO_2 for water splitting reaction were investigated. The Ag_2O/TiO_2 catalyst contained 28% of silver and 72% titanium by w/w and XPS and XRD results revealed the presence of $Ag_2O(Ag^+)$, Ag^o, $TiO_2(Ti^{4+})$ and Ti^{3+} states in Ag_2O/TiO_2 catalyst. A solid proof for the IR photon initiated catalytic activity of Ag_2O/TiO_2 catalyst was observed from the clear enhanced IR response in the incident photon current conversion efficiency measurements of the Ag_2O/TiO_2 catalyst. Considering the band gap energies to the energy of the IR source, Plasmon assisted photocatalytic activity and/or a sub-band gap phonon-assisted multi-photon excitation mechanisms are proposed for the observed infrared photocatalytic activity of Ag_2O/TiO_2 photocatalyst and functions of Ag_2O and TiO_2 in "dark photocatalysis" are discussed.

1. Introduction

Conversion of solar energy into chemical fuels such as hydrogen is highly encouraged and it is an important area of research.[1-3] Secondly, hydrogen is a valuable product as a potential fuel and an energy carrier. It is non-polluting, renewable, inexhaustible and very flexible with respect to conversion to other forms of energy (i.e. heat via combustion or electricity via fuel cells).[4] Finally, hydrogen is valuable in its own right as a basic chemical feedstock used in large quantities for ammonia synthesis and petroleum refining. Production of hydrogen by electrochemical photolysis of water by single-crystal TiO_2 under UV light was first reported with analogy to natural photosynthesis in 1972.[1] Since then, intensive research on conversion of solar energy into hydrogen energy was carried out using photoelectrochemical systems [5-7] as well as photocatalytic systems.[8-10] In either case, TiO_2 is the most widely used photocatalytic material [11]. Though TiO_2 is a highly stable photocatalyst with appropriate energy positions for water splitting reaction,[12, 13] practical use of TiO_2 is limited as it absorbs mainly high energy photons in the UV region of the solar spectrum.[14, 15] Band gap engineering is a widespread method that has been employed to alter the band gap energy and many attempts have been made to utilise the visible region of the solar spectrum of TiO_2 photocatalysts through impurity doping, metallisation and sensitization.[16-18]

However, successful methods have not been reported to use the IR region of the solar spectrum for photolysis of water. Advantage of such a system is that IR waves are available from the sunset to sunrise and the solar spectrum consists of 47% IR radiation.[19] Hence, finding novel nanostructured semiconductors that would absorb lower-energy photons such as visible and infrared (IR) regions of the solar spectrum is imperative for pragmatic applications of photocatalysts. Even though there are no reports on photocatalysts that utilizes entirely IR photons, near IR active photocatalysts such as Bi_2WO_6,[20] NaYF4:Yb,Tm@TiO_2,[21] $Cu_2(OH)PO_4$,[22] have been reported. The Ag_2O/TiO_2 photocatalytic system which absorbs low-energy photons and generates active electron-hole (e^--h^+) pairs resulting in H_2 generation in water and water/methanol solution was reported recently.[23] In the Ag_2O/TiO_2 photocatalytic system, TiO_2 was used as a supporting materials and silver and silver oxide as light harvesting materials due to generation of optical near field and surface plasmon by Ag/Ag_2O. In this investigation, we discuss the material aspects and the photocatalytic mechanism of the Ag_2O/TiO_2 photocatalyst in detail. For the observed photoactivity of Ag_2O/TiO_2 catalyst in the IR region, two possible mechanisms are proposed.

2. Results and discussion

2.1 Characterization of catalyst

[a] Institute of Fundamental Studies, Hantana Road, Kandy, CP 20000, Sri Lanka
[b] Email: bandaraj@ifs.ac.lk; jayasundera@yahoo.com

Crystalline structure and oxidation states of Ag and Ti in the Ag_2O/TiO_2 catalyst were identified by XRD and XPS analysis which confirmed the presence of Ag^0, Ag_2O, $Ti^{4+}(TiO_2)$ and Ti^{3+} in the catalyst. Crystallinity and the crystalline phase of the Ag_2O/TiO_2 heterostructures were analysed using XRD and the X–ray diffraction patterns of P25 TiO_2 and Ag_2O/TiO_2 heterostructure (before and after irradiation) are shown in Fig. 1. In Fig. 1, the characteristic peaks of pure P25-TiO_2 corresponding to anatase and rutile phases can be detected (JCPDS anatase #, No.78-2485). Similarly, in the Ag_2O/TiO_2 structure, in addition to diffraction peaks corresponding to P25 TiO_2, diffraction peaks corresponding to hexagonal Ag_2O (100) and (011) planes at 33.6° and 38.39° respectively (JCPDS No.72-2108) and a peak for cubic Ag_2O were also detected at 32.56° (JCPDS No.76-1393). Also AgO diffraction peak at ~ 31.3° (002) is clearly noticeable. Additional diffraction peaks corresponding to Ag^0 was also detected at 38.11° (111) and 77.29 (311) (JCPDS No.76-1393) [24]. Furthermore, the sharp diffraction peak of Ag_2O nanoparticles in the Ag_2O/TiO_2 heterostructure indicates the high degree of crystallinity of Ag_2O in Ag_2O/TiO_2structure. The peak at 48˚ in Fig.1 (b) is due to presence of unreacted trace amount of $AgNO_3$(JCPDS 43-0649) and the peak disappears upon IR irradiation (Fig. 1(c)) as $AgNO_3$ converts to Ag upon irradiation. It was noted that the $AgNO_3$ peak does not appear in all samples and also it does not affect the catalytic activity as it readily converts to Ag/Ag_2O and disappear after irradiation ($AgNO_3$ peak marked as *in diffraction pattern b is not seen in the diffraction pattern of c.

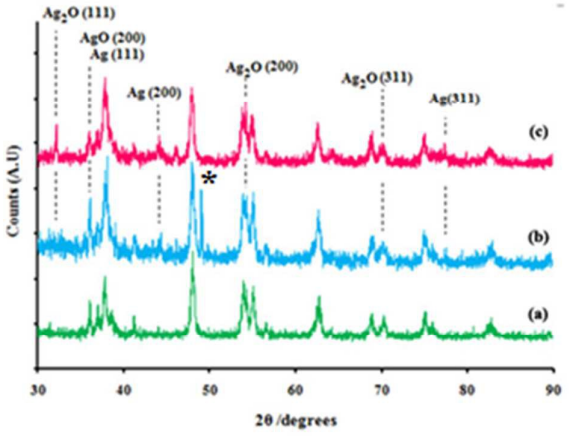

Figure 1: XRD patterns of (a) TiO_2, (b,c) Ag_2O/TiO_2 photocatalyst before and after IR irradiation respectively.

It is interest to note the appearance of blue colour of the catalyst Ag_2O/TiO_2 when the catalyst is prepared in the presence of light (visible or IR light under diffuse day light) and absorption spectra of the catalysts prepared under light and dark conditions are shown in Fig. 2. Inset in Fig. 2 shows the images of catalyst prepared under light (image a) and dark (image b) conditions. The appearance of blue colour in Ag_2O/TiO_2 could be due to formation of reduced Ti^{3+} states in Ag_2O/TiO_2 catalyst and the formation of Ti^{3+} states can be understood as follows; during the catalyst preparation process, Ag^+ get adsorbed on to TiO_2 surface and converted to Ag_2O with the addition of NH_3. Once Ag_2O is formed on TiO_2 surface, it can generate excited e^--h^+ pairs by absorbing diffuse light and consequent transfer of excited electrons from Ag_2O to TiO_2 form blue colour in the Ag_2O/TiO_2 catalyst due to trapped electrons in (TiO_2-e^-).[25-27]

$$Ag_2O \rightarrow Ag_2O(e - h^+) \quad (1)$$

$$TiO_2/Ag_2(e - h^+) \rightarrow TiO_2(e -)/Ag_2O(h^+) \quad (2)$$

As shown in reactions (1) and (2), photogenerated electrons are trapped at hydroxylated surface titanium and these electrons believed to be trapped at surface Ti^{4+}(OH) centres forming blue interstitial Ti^{3+} lattice [25, 26].

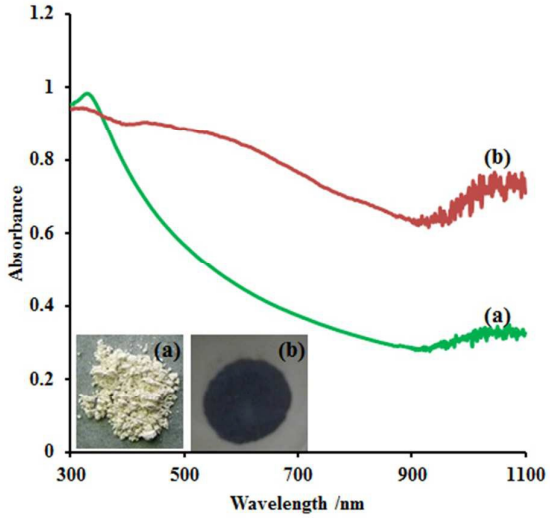

Figure 2: UV-VIS spectrum of Ag_2O/TiO_2 photocatalyst prepared under (a) dark and (b) ambient conditions.

It is well known that the reduced Ti^{3+} sites are readily converted to Ti^{4+} sites through atmospheric oxidation. However, the blue colour of the Ag_2O/TiO_2 catalyst remains stable even under air saturated condition and the persistent blue colour in the Ag_2O/TiO_2 photocatalyst indicates that these reduced sites are created continuously owing to the activity of diffuse visible/IR radiations. The formation of reduced Ti^{3+} state in Ag_2O/TiO_2 catalyst is confirmed by XPS data shown in Fig. 3. XPS data of as prepared Ag_2O/TiO_2 photocatalyst given in Fig. 3a has two Ti2p peaks at 459.4 eV and 464.9 eV arising from the Ti^{4+} state and the peaks at 457.8 eV and 462 eV arising from the Ti^{3+} state [25, 28, 29]. On the other hand, the XPS results of authentic samples of TiO_2 given in Fig. 3b shows only Ti 2p peaks at 459.4 and 464.9eV corresponding to Ti^{4+} state. As the additional Ti 2p peaks seen in Ag_2O/TiO_2 photocatalystcorrespond to Ti^{3+} sites, it can be concluded that both Ti^{4+} and Ti^{3+} states are present in the Ag_2O/TiO_2 photocatalyst and confirm that the observed blue colour in Ag_2O/TiO_2 photocatalyst is due to presence of reduced Ti^{3+} in

the Ag_2O/TiO_2 catalyst. The XPS of the Ag peaks of the Ag_2O/TiO_2 catalyst before and after IR irradiation are shown in Fig. 3c and 3d respectively. As shown in Fig. 3c, appearing of slightly shifted Ag $3d_{3/2}$ peaks at 374, 375 and 378 eV are due to Ag^+ and Ag^0 states respectively indicating the presence of both Ag^+ and Ag^0 states in the Ag_2O/TiO_2 photocatalyst[30-32]. The additional peaks seen in the sample before irradiation at 371.1 and 377.1 eV could be due to a charge transfer transition in Ag^{3+} (or due to unreacted $AgNO_3$) which is found to be disappeared upon irradiation (Fig. 3d) [33]. It is also noted the decrease of the Ag^o/Ag^+ peak intensity ratio after irradiation and the decrease of Ag^0 peak intensity with the concomitant increase in Ag^+ peak upon IR irradiation could be due to photooxidation of some of the Ag^0 ions in to Ag_2O.

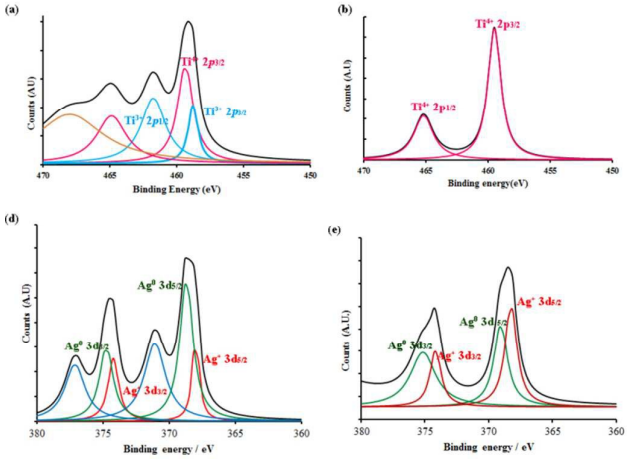

Figure 3: XPS spectra of Ti 2p of (a) Ag_2O/TiO_2 photocatalyst, (b) TiO_2 and the Ag 3d of (c,d) Ag_2O/TiO_2 photocatalyst before and after IR irradiation respectively.

TEM micrographs were obtained in order to obtain the morphology, particle size, crystallographic structure and the material composition of the Ag_2O/TiO_2 photocatalyst. The TEM images and the lattice fringes of the Ag_2O/TiO_2 catalyst are shown in Fig. 4a and b respectively. It can be seen that there are three distinguishable particle types appear in these micrographs which are due to TiO_2, Ag_2O and Ag nanoparticles. The TEM images further evidence that the black colour particles (intended to be Ag_2O) and light colour particles (TiO_2) are in similar order of size while another set of particles are in the quantum dot size which could be due to Ag^0 particles. The magnified TEM image of the Ag_2O/TiO_2 photocatalystin 10 nm scale is shown in Fig. 4b and the particles with fringe widths of 0.27 nm and 0.24 nm seen in Fig. 4b confirms the presence of Ag_2O [111] and [200] planes of Ag_2O [34, 35]. On the other hand, the particles with fringe width of 0.35 nm can be attributed to TiO_2 anatase [101] lattice plane [34, 35]. The~1 -10 nm particles seen in Fig 4 may also could be due to Ag_2O. As Ag_2O and Ag are interconvereted upon irradiation hence the dark coloured particles could be due to Ag/Ag_2O heterostructure.

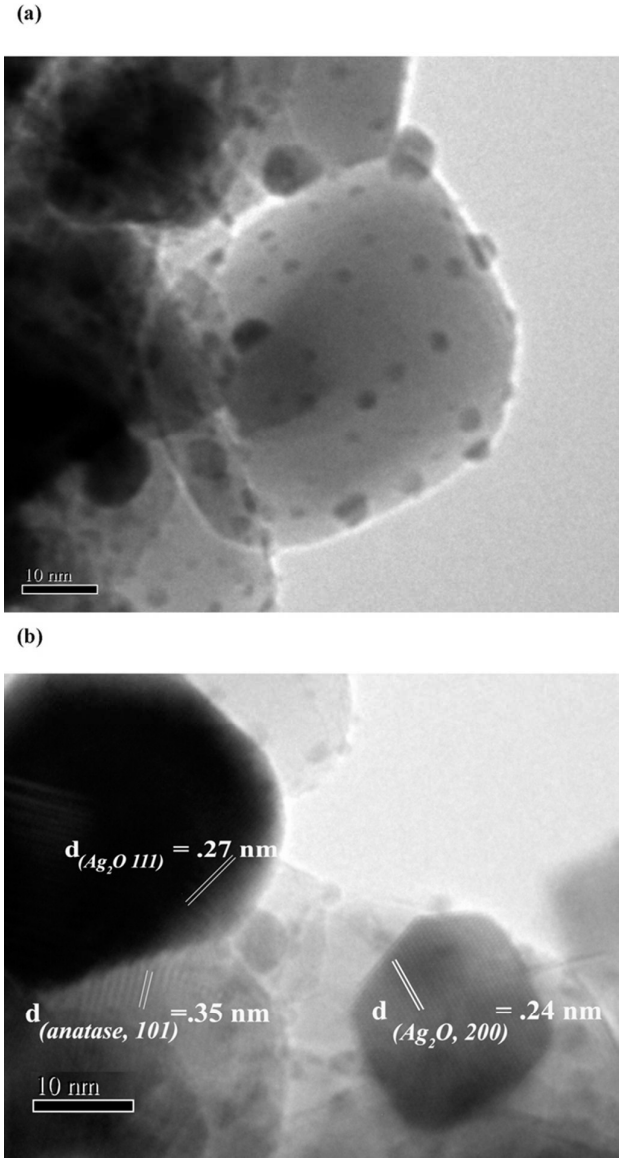

Figure 4: (a) TEM image and (b) Crystal lattice fringe image of Ag_2O/TiO_2 photocatalyst.

Figure 5 shows the optical properties of Ag_2O, TiO_2 and Ag_2O/TiO_2. Also shown in Fig. 5 is the absorption spectrum of Ag_2O/TiO_2 photocatalyst after IR irradiation of the catalyst for comparison purpose. The bare TiO_2 shows absorption around 400 nm regions with an absorption threshold at ~380 nm due to direct band gap excitation. In the absorption spectrum of Ag_2O, the electronic transitions of metallic Ag^0 appear in the 250-330 nm spectral range while a weak Ag plasmon peak is seen in the visible region. Furthermore, absorption rise seen in the IR region in Fig. 5 could be due to the direct band gap excitation of Ag_2O. The UV-VIS absorption spectrum of as prepared Ag_2O/TiO_2 shows a featureless absorption starting

from ~700 - 800 nm with clear absorption peaks around 380 and 280 nm due to Ag^0 and TiO_2. However, just after irradiation with IR radiation in the presence of water, the catalyst turns to a black colour with broad absorption peaks appearing at 350, 410, 550 and 800 nm where peak at 410 nm is due to surface plasmonic resonance of silver and the peaks seen at ~550 and 850 nm can be attributed to Ag_2O absorptions. Considering direct band gap excitation of Ag_2O at 850 nm, a band-gap value of approximately 1.58 eV was determined and the value agrees well with the reported band gap *E* of ~1.5 eV for Ag_2O [36, 37].

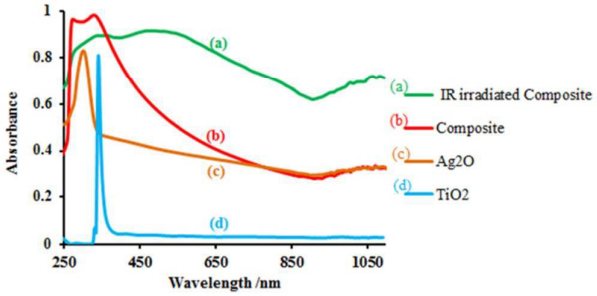

Figure 5: UV-VIS spectrum of (a) IR irradiated Ag_2O/TiO_2photocatalyst, (b) Ag_2O/TiO_2photocatalyst before irradiation, (c) Ag_2O and (d) TiO_2

2.2 Mechanism of Ag_2O and Ag^0 formation during catalyst preparation

By XPS, XRD and TEM analyses, it was shown the presence of Ag^0 and Ag_2O in Ag_2O/TiO_2 structure and the formation of Ag^0 and Ag_2O in the Ag_2O/TiO_2 photocatalyst can be described as follows [11, 30, 38-40].

$$Ag^+ + OH^- \rightarrow AgOH \qquad (3)$$

$$2\,AgOH \rightarrow Ag_2O + H_2O \qquad (4)$$

$$Ag_2O \xrightarrow{h\nu} AgO + Ag^0 \qquad (5)$$

$$AgO \rightarrow Ag^0 + {}^1/_2\,O_2 \qquad (6)$$

In the first step, AgOH is formed on the surface of TiO_2 by the addition of hydroxyl ions to TiO_2/Ag (adsorbed). The AgOH readily decomposes to form Ag_2O and in the presence of light, Ag_2O tends to form Ag^0 and AgO (reactions 4 and 5). As AgO is highly unstable, it is rapidly decomposes to Ag^0 (reaction 6).

2.3 Photocatalytic activity

Photocatalytic activities of Ag_2O/TiO_2 under UV and visible light have been reported already.[41, 42] In this investigation, hydrogen production of Ag_2O/TiO_2, individual catalysts of TiO_2 and Ag_2O were examined under IR irradiation with pure water and 10% methanol solution under air and argon saturated conditions. As control experiments, hydrogen production was investigated with similar conditions described above under dark conditions. The hydrogen production rates under air and argon saturated conditions are shown in Fig. 6a while Fig. 6b shows the hydrogen production rates of pure water under air and argon saturated conditions. As shown in both Fig. 6a and 6b, when the catalyst $Ag_2O/TiO_2$was irradiated with IR source in both 10% methanol solution and water, production of hydrogen was noticed. (The H_2 production rates reported in this investigation is comparatively low and cannot be compared with the literature reported H_2 production rates as we have used very low intensity IR radiation of 3.2 mW cm^{-2}). Additionally, less than 0.005 ml $h^{-}1g^{-1}$ of hydrogen production rate was observed when the irradiations were carried out only with Ag/Ag_2O or TiO_2 catalysts under similar photolysis conditions where the real H_2 production rates of these conditions are discussed later. Also hydrogen production was not observed without the catalyst and under dark in the presence of Ag_2O/TiO_2 catalyst (Fig. 6c). The spectrum of the IR source (measured from Ocean optics QE65 Pro spectrometer) shown in the Fig. 6d, confirms that the IR light source mainly emits radiation in the 800 – 1000 nm region. These observations confirm the IR photon activated catalytic activity of the Ag_2O/TiO_2 catalyst.

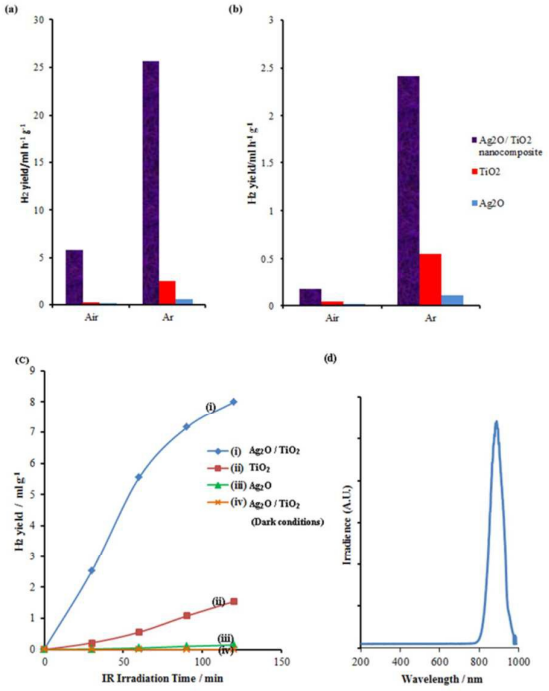

Figure 6: H_2 production rateby photolysis of (a) 10% methanol and (b) deionised water only at Ar saturated and air saturated conditions under IR irradiation (3.2 mW cm^{-2}). (c) The H_2 production rate at different irradiation time under air saturate conditions under IR irradiation (3.2 mW cm^{-2}) and (d)the spectrum of the IR lamp source.

The observed hydrogen production rates of Ag_2O, TiO_2 and Ag_2O/TiO_2 in 10% methanol solution under air saturated conditions with IR light source (850 nm) were 0.17, 0.19 and

5.83 ml h^{-1} g^{-1} respectively while for the same systems, 0.56, 2.41 and 25.64 ml $h^{-1}g^{-1}$ hydrogen production rates were observed under argon saturated condition. A lower hydrogen production rate under air saturated conditions is mainly due to capture of photogenerated electron by oxygen. At the same time, 0.11, 0.55 and 2.41 ml h^{-1} g^{-1} hydrogen production rates were observed for Ag_2O, TiO_2 and Ag_2O/TiO_2 respectively when the irradiation was carried out with water. A similar H_2 production rates were observed for the catalytic systems described above with a 950 nm IR emitting diode. Hydrogen production rates under IR irradiation with the pure water and 10% methanol indicate an enhanced hydrogen production rate with 10% methanol. A higher production rate of hydrogen with methanol can be explained considering the photocatalytic mechanism. According to the photocatalytic water splitting reaction mechanism [11], photogenerated electrons and holes participate for water reduction and oxidation producing H_2 and O_2 respectively. Adding electron donors (sacrificial reagents or hole scavengers) enhance the photocatalytic electron/hole separation resulting in higher quantum efficiency. As methanol is a better sacrificial agent than H_2O, a higher production rate of H_2 with water/methanol can be justified. It was noted that the hydrogen production rate of the Ag_2O/TiO_2 catalyst with IR irradiation is highly depended on pH of the solution. H_2 production rates of Ag_2O, TiO_2 and Ag_2O/TiO_2 in 10% methanol solution at pH 7 were 0.56, 2.41 and 25.64 ml h^{-1} g^{-1} respectively under IR light source (3.2 mW cm^{-2}). H_2production rates of Ag_2O/TiO_2 in 10% methanol increases to 41.06 ml h^{-1} g^{-1} when the pH of the medium is 9 and the H_2production rate slightly reduces to 22.2 ml h^{-1} g^{-1} when the pH of the solution is 4. During irradiation with different pH values, only a slight change in pH values in the irradiation solutions was noticed. Furthermore, no hydrogen was observed when the photolysis was carried out in absolute methanol. To demonstrate that the Ag_2O/TiO_2photocatalyst exhibits stability and sustained activity for the photocatalytic hydrogen production from water under IR irradiation, photolysis was carried out for four consecutive cycles with one cycle lasting for two and half hours and the results are shown in Fig. 7. It is evident that in each catalytic cycle, the Ag_2O/TiO_2 catalyst produces equal amounts of hydrogen gas indicating the stability of the catalyst.

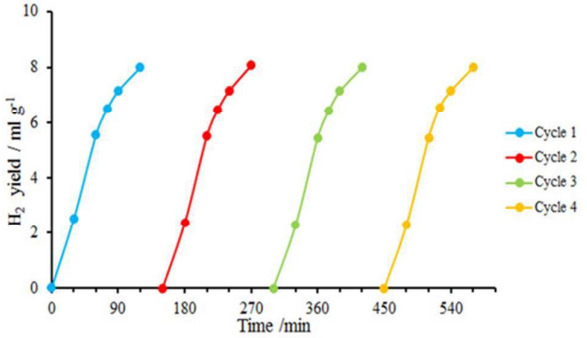

Figure 7: Photocatalytic H_2 production from 10% methanol under IR irradiation, photolysis was carried out for four consecutive cycles under air saturate conditions.

2.4 Reaction mechanism

As the irradiation light source for the above experiments was either 850 or 950 nm light emitting IR diodes, it can be assumed that the photolysis of water with Ag_2O/TiO_2 catalyst is initiated by the absorption of IR photons. A higher hydrogen production rate with Ag_2O/TiO_2 catalyst than that of Ag_2O or TiO_2 alone indicates the existence of a synergic effect of both TiO_2 and Ag_2O in IR initiated catalytic activity of the Ag_2O/TiO_2 catalyst. The spectral response measurement or Incident Photon to Current Efficiency (IPCE) measurements of Ag_2O/TiO_2 catalyst shown in Fig. 8 clearly demonstrates the IR response of the catalyst in the 700-1300 nm regions. As shown in Fig. 8, the IPCE spectrum of Ag_2O/TiO_2 shows a wide response from 300-1100 nm with clear two responses at 350 and 850 nm. The sharp response at 350 nm corresponds to the direct excitation of electrons from VB to the CB of TiO_2. The broad response in the visible-IR region could be easily assigned to the excitation of silver resonance plasmon and Ag_2O particles by comparing the IPCE spectra of individual TiO_2, Ag_2O with Ag_2O/TiO_2 shown in Fig. 5. The broad spectral response in the VIS-IR region with a sharp response at ~850 nm indicates that the observed broad response of Ag_2O/TiO_2 in VIS-IR regions arises due to Ag and Ag_2O. Hence, we propose two possible reaction mechanisms; (a) tuneable surface Plasmon resonance of Ag/Ag_2O or (b) Optical Near Field (ONF) induced – phonon assisted IR response.[43-46]

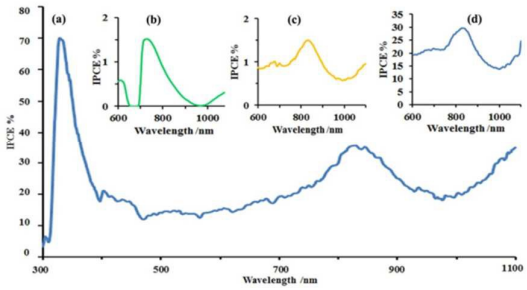

Figure 8: IPCE of the cells, (a,d) Ag_2O/TiO_2 photocatalyst, (b) TiO_2, (c) Ag_2O in 10% methanol electrolyte and the platinum counter electrode at bias voltage of 200 mV.

It is known that the silver Plasmon can be extended to IR and NIR regions.[47, 48] As such, in the tuneable surface plasmon mechanism, it can be assumed that Ag/Ag_2O plasmon can absorb single IR photon generating e-h pairs in Ag/Ag_2O [47, 48] and consequence transfer of excited electron to the CB of TiO_2. The injected electrons in TiO_2 can be trapped in shallow and deep trap states situated at 0.1 and 0.8 eV respectively below the CB of TiO_2 forming Ti^{3+} states. These trapped electrons can be re-excite to the CB by the absorption of IR radiation [49, 50] as shown schematically in Fig. 9a. In the second mechanism, a phonon assisted multi-photon catalytic system is proposed as shown in Fig. 9b and can be explained as follows. By considering the band gap energies of TiO_2 (3.2 eV) and Ag_2O (1.58 eV), it can be inferred that the direct band gap excitation is not possible with 850 nm or 950 nm IR diodes as their

energies 1.45 and 1.30 eV respectively are not sufficient to excite electron from the valence band (VB) to the conduction band (CB) of both TiO_2 and Ag_2O. As explained before, the observed IR response of Ag_2O/TiO_2 catalyst cannot be assigned to direct band gap excitations by IR source due to insufficient energy of the IR radiations. Instead excitation should occur via sub-band gap or multi-photon excitation.[45, 46, 51, 52] Multi-photon excitations have been reported for several oxides[53-55] and nitrides[56] and the observed multi-photon excitation has been attributed to optical near field (ONF) induced – Phonon assisted sub-band gap response.[57]

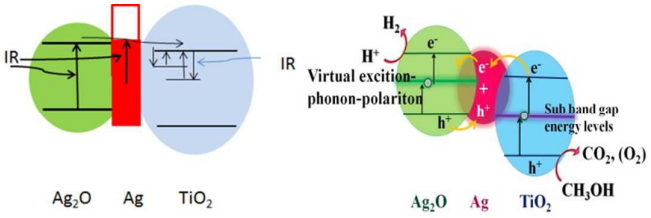

Figure 9: Schematic energy diagram of proposed photocatalytic process of $Ag_2O/Ag/TiO_2$ photocatalyst (a) tuneable surface Plasmon resonance of Ag/Ag_2O and (b) Optical Near Field (ONF) induced – phonon assisted IR response.

To confirm the multi-photon excitation, we studied the excitation intensity dependence on the H_2 production rates of the Ag_2O/TiO_2 photocatalyst and the results are shown in Fig. 10a. As shown in Fig. 10a, the hydrogen yield is increased exponentially with the increase of light intensity and the exponential increase in hydrogen yield is mainly due to non-linear excitation process in IR initiated light reaction. As shown in the inset in Fig. 10a, the plot of ln[H_2 production rate] vs, ln(Intensity) gave a slope of 1.78 further substantiating that the reaction proceeded via a non-linear process that involves multi-photon or step-wise multiphoton electron excitation [58].

To further substantiate the multi-photon process, we investigated the initial voltage response time of an electrode fabricated with Ag_2O/TiO_2 film on FTO substrate. For voltage response study, a mixture of 10 % MeOH and 0.01 KCl was used as the electrolyte and Pt as counter electrode, voltage response was measured by varying the excitation light source and excitation wavelengths. As shown in Fig. 10b and 10c, when illumination was carried out either with standard AM 1.5, 1.0 or 0.3 sun conditions, a rapid V_{oc} response was noticed due to direct band gap excitation of electron from VB to the CB. However as shown in Fig. 10d, when the illumination was carried out with 880 nm IR diode, only a slow V_{oc} response was noticed. The standard AM 1.5 light source consists of UV lights as well as visible region in the 300-800 nm regions while IR diode emits photons at 950 nm. Hence, a sharp V_{oc} response observed when the Ag_2O/TiO_2 system is irradiated with standard light source can be understood on the basis the excitation radiation provides sufficient energy to excite electrons from the VB to the CB. However, in the case of IR irradiation, since excitation radiation does not provide sufficient energy to excite electrons directly from VB to the CB, a slow V_{oc} rise was noted due to filling of sub-band gaps. It is also interesting to point out that it is not possible to fit the V_{oc} data for IR irradiated electrode in Fig. 10d with a single exponential function and needs a multiple exponential model indicating that the IR excitation process is likely to be a multiple step process.

All these results strongly evident the IR initiated photocatalytic activity of Ag_2O/TiO_2 photocatalytic system. However, we noticed that sonication is needed throughout the experiment to separate the photoproduced hydrogen gas as it re-adsorb or react if sonication is not present. One could argue that H_2 could produce via sonochemical reaction of water-methanol mixture as it is known the production of H_2 via sonochemical reaction[59]. When sonication was carried out for water-methanol mixture without catalyst and under air with no light, the observed H_2 yield is 0.005 ml h^{-1} which is ~1000 times less than the presence of Ag_2O/TiO_2 photocatalyst and IR radiation suggesting that the IR activity of the catalyst. Furthermore, we have demonstrated the exponential increase in H_2 production rate with the increase of IR light intensity while keeping the sonication at the same level (Figure 10a). If the H_2 production is mainly due to sonochemical reaction, the observed dependence of H_2 yield with the IR light intensity could not be observed indicating that the H_2 production is mainly due to IR initiated photocatalytic activity of Ag_2O/TiO_2 system and the following reaction mechanism is proposed.

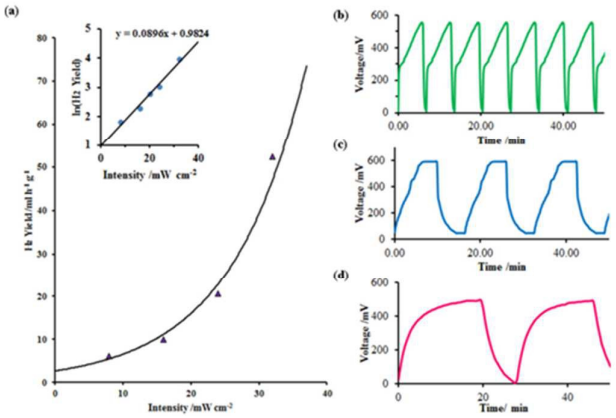

Figure 10: (a) H_2 production rate at different IR intensities. Inset in Figure 9(a) is the plot of ln [H_2 production rate] Vs. ln (Intensity) and the voltage rise curve with Irradiation time (b) and (c) under 1 and 0.3 Sun intensity of the solar simulator respectively and (d) under IR irradiation.

In the proposed ONF-phonon assisted process, the ONF generated at the nanostructures could excite the coherent phonons in the nanostructures forming virtual excition-phonon-polariton as shown in Fig. 9b [45]. These quasi particles can excite the electrons to the phonon level and successively to the CB. This type of multi-step excitation process is possible even the incident photon energy is lower than the band gap energy. As explained earlier, Ag^0 and Ag_2O can generate phonons as well as ONF upon IR illumination as they are well known to generate plasmon as well as ONF [36, 43, 44, 57, 58]. These

ONF with the assistance of phonons could generate exciton-phonon-polariton in both TiO_2 and Ag_2O. As the energy required for the process is very low, IR radiation can excite electrons from VB of both TiO_2 and Ag_2O to these sub energy levels as shown in Fig. 9b and with a sequence of steps, an electron will be excited from VB to the CB of both TiO_2 and Ag_2O. Such an approach requires the existence of proper electronic states whose energy positions lie within the band gap. These states could be the localized electronic states (LS) of intrinsic defects[57]. Once electrons and holes are generated in CB and VB respectively by the IR irradiation, these photogenerated charges in Ag_2O and TiO_2 can be separated easily in the $Ag_2O/Ag/TiO_2$ catalyst owing to formation of a p-n junction. As discussed earlier, the catalyst consists of $Ag_2O/Ag/TiO_2$ structure and being Ag_2O and TiO_2 p and n type semiconductors respectively, they form p-metal-n junction. Due to large work function of silver, the photoexcited charges are easily take up by Ag^0 and photoexcited electrons in TiO_2 and photogenerated holes in Ag_2O could travel to ohmic-contact of Ag^o and get recombined. Additionally, due to large work-function of Ag^o and favourable band energy positions of TiO_2 and Ag_2O, it would be possible to transfer of electrons from TiO_2 and holes from Ag_2O to the ohmic contact of TiO_2-Ag^o-Ag_2O resulting in an efficient charge separation of photogenerated holes and electron in TiO_2 and Ag_2O respectively. The photoexcited electrons of Ag_2O could easily migrate to the water-Ag_2O interface where they can participate for the water splitting reaction producing H_2 as the CB energy of Ag_2O -1.7eV (Vs. NHE at pH7) is energetic for water reduction reaction. Likewise, photogenerated holes in TiO_2 can be transferred into water-TiO_2 interface and participate of oxidation reaction as the VB of TiO_2 2.58 eV(Vs. NHE at pH7) is energetic enough for oxidation reaction [34, 60-63]. The proposed IR active photocatalytic system for the production of H_2 could be a promising artificial system for efficient harvesting of solar energy, especially the IR region of the solar spectrum. The present IR photon harvesting system can be applied not only for the photolysis of water but also for photodegradation of pollutants and conversion of solar energy into electrical energy.

Considering all these observations, the IR initiated catalytic activity of Ag_2O/TiO_2 photocatalyst could be mainly assigned to sub-band gap filling as it involves a multi-photon process as well as trapping and de-trapping of electrons and holes created by IR photon excitation [45, 46, 51, 52]. However, we cannot totally exclude the surface Plasmon initiated reaction mechanism and hence further experiments are needed to distinguish the proposed reaction mechanisms.

3. Experimental

3.1 Preparation of photocatalyst: TiO_2 (Degussa P25) was used as the source of TiO_2 nanoparticles. $AgNO_3$, 33% ammonia solution and 99% methanol were BDH analytical grade chemicals and used as received. A mixture containing TiO_2 (2% w/v) in 50 ml of 0.04 M aqueous $AgNO_3$ was stirred for 30 minutes followed by the addition of a *stoichiometric* amount of 33% ammonia solution for the complete conversion of $AgNO_3$ to Ag_2O. The resulting mixture was heated at 150^0C until the product is completely dry and the resultant powder was calcined at 250^0C for 30 minutes. TiO_2 catalyst without Ag_2O and Ag_2O without TiO_2 were also prepared in a similar manner without adding $AgNO_3$ and TiO_2 respectively and taken as control catalysts.

3.2 Characterization of catalyst:SEM image was recorded with Hitachi SU6000 FESEM and TEM image was recorded from FEI Tecnai F-20, 200keV scanning transmission electron microscopy. XPS was taken from hemispherical electron energy analyser (ESCALAB-MkII, VG) and an Al K X-ray tube (1486.6 eV). UV visible spectrum was recorded in ShimadzuUV-2450 UV-VI spectrophotometer. For absorption measurements, the catalysts powders were dispersed in water and spectra were recorded against water reference. XRD was taken from SEIMENS (D5000) X-ray diffractometer with Cu anode, Ni filter at 1.54 Å. External incident photon current conversion efficiency (IPCE) was measured using a Bentham PVE 300 1700 IPCE apparatus. For V_{oc} analysis, a photovoltaic cell was prepared with Ag_2O/TiO_2 paste using the doctor blade method. Few drops of a paste made from 25 mg of Ag_2O/TiO_2 photocatalyst in 2.5 ml deionized water was placed on cleaned FTO and spread by doctor blade method followed by drying at 105^0 C and sintered at the same temperature for further 15 minutes. Ag_2O/TiO_2 coated FTO electrode and a Pt counter electrode were fixed together and 10% methanol and 0.01 M KCl electrolyte was filled using the capillary action. The photovoltaic cell was irradiated with IR emitting diodes (3.2 mW cm^{-2}) and the voltage was recorded until it rises to a steady value. Then the IR source was switched off and the voltage decay was recorded with time.

3.3 Photolysis experiment and product analysis: For the photolysis experiment, finely ground 12.5 mg of Ag_2O/TiO_2 photocatalyst was dispersed in 20 ml of 10% methanol or deionised water and placed in a 25 ml borosilicate flask which is tightly sealed with a gas septum. The reaction was carried out in a borosilicate vessel while irradiating either with 850 or 950 nm IR emitting diodes (ϕ 5mm) and the experiments were carried out in a dark room to avoid UV and visible light. Prior to irradiation, the system was thoroughly purged with Ar for 1 hr when the photolysis was carried out in O_2 free environment or otherwise the irradiation was done under normal atmospheric conditions. Prior to irradiation, the flask with catalyst (neatly covered with aluminium foil) was sonicated for 30 minutes in a dark room. In a separate experiment, the photolysis experiments were carried out with TiO_2, Ag_2O and Ag_2O/TiO_2 catalysts in the presence of distilled water alone. The gases products were quantitatively analysed using a Shimadzu gas chromatograph GC-9AM with TCD detector with a packed charcoal column using Ar as the carrier gas where the sensitivity of the detector is 7000 mV, ml/mg. For the calculation of hydrogen production rates, the total amount of hydrogen produced for different time intervals were calculated against the hydrogen calibration plot. Throughout the experiment, the system was subjected to sonication to separate H_2 from the catalyst surface as Ag_2O /TiO_2 catalyst

adsorbs produced hydrogen rapidly. Control experiments were carried out with IR source in the absence of catalysts and without IR source in the presence of catalysts.

4. Conclusions

The Ag_2O/TiO_2 photocatalyst consists of 28% of silver and 72% titanium by w/w and the presence of oxidation states of Ag^+, Ag^o, Ti^{4+} and Ti^{3+} were confirmed by XPS analysis. Persistent presence of Ti^{3+} states in Ag_2O/TiO_2 catalyst is noticed during photochemical reaction and confirms the continuous formation of reduced state of Ti^{3+} during light reaction. The Ag_2O/TiO_2 photocatalystin water and water/methanol mixture produces hydrogen when irradiated with IR photons. For the observed photocatalytic activity, two possible reaction mechanisms are proposed; (a) tuneable surface Plasmon resonance of Ag/Ag_2O or (b) Optical Near Field (ONF) induced – phonon assisted IR response. In the proposed multi-photon process, the generation of phonons as well as ONF on Ag^0 and Ag_2O generating virtual excition-phonon-polariton upon IR illumination could play a significant role. These quasi particles can excite the electrons to the phonon level and successively to the CB. Additionally, p-n junction formed by Ag_2O and TiO_2 together with the ohmic contact with Ag layer may enhance the separation of photogenerated charge carriers in Ag_2O/TiO_2 photocatalyst. Also, observed IR photocatalytic activity of Ag_2O/TiO_2 may also be initiated by the surface Plasmon absorption and hence further experiments are needed to distinguish the proposed reaction mechanisms.

Acknowledgements

The acknowledgements come at the end of an article after the conclusions and before the notes and references. Financial support from NRC, Sri Lanka (NRC 07 – 46) is highly appreciated. It should be a pleasure of acknowledge Prof. Mowafak Al-Jassim (NREL, Colorado,USA) for providing SEM and TEM images. We wish to thank Ms. Darshani Aluthpatabendi for the technical assistance given during this study.

Notes and references

1. A. Fujishima, *Nature*, 1972, **238**, 37-38.
2. C.-J. Lin, Y.-T. Lu, C.-H. Hsieh and S.-H. Chien, *Applied Physics Letters*, 2009, **94**, 113102.
3. M. R. Hoffmann, S. T. Martin, W. Choi and D. W. Bahnemann, *Chemical reviews*, 1995, **95**, 69-96.
4. C. W. Dunnill, Z. Ansari, A. Kafizas, S. Perni, D. J. Morgan, M. Wilson and I. P. Parkin, *Journal of Materials Chemistry*, 2011, **21**, 11854-11861.
5. O. Khaselev and J. A. Turner, *Science*, 1998, **280**, 425-427.
6. T. Bak, J. Nowotny, M. Rekas and C. Sorrell, *International journal of hydrogen energy*, 2002, **27**, 991-1022.
7. J. R. Bolton, *Solar Energy*, 1996, **57**, 37-50.
8. X. Chen, S. Shen, L. Guo and S. S. Mao, *Chemical Reviews*, 2010, **110**, 6503-6570.
9. Z. Zou, J. Ye, K. Sayama and H. Arakawa, *Nature*, 2001, **414**, 625-627.
10. H. Yan, J. Yang, G. Ma, G. Wu, X. Zong, Z. Lei, J. Shi and C. Li, *Journal of Catalysis*, 2009, **266**, 165-168.
11. M. Ni, M. K. Leung, D. Y. Leung and K. Sumathy, *Renewable and Sustainable Energy Reviews*, 2007, **11**, 401-425.
12. J. Bandara, C. Udawatta and C. Rajapakse, *Photochemical & Photobiological Sciences*, 2005, **4**, 857-861.
13. K. Hashimoto, H. Irie and A. Fujishima, *Japanese journal of applied physics*, 2005, **44**, 8269.
14. A. L. Linsebigler, G. Lu and J. T. Yates Jr, *Chemical reviews*, 1995, **95**, 735-758.
15. Y. Gai, J. Li, S.-S. Li, J.-B. Xia and S.-H. Wei, *Physical review letters*, 2009, **102**, 036402.
16. K. Lalitha, G. Sadanandam, V. D. Kumari, M. Subrahmanyam, B. Sreedhar and N. Y. Hebalkar, *The Journal of Physical Chemistry C*, 2010, **114**, 22181-22189.
17. K. Nagaveni, M. Hegde, N. Ravishankar, G. Subbanna and G. Madras, *Langmuir*, 2004, **20**, 2900-2907.
18. C. B. Almquist and P. Biswas, *Journal of Catalysis*, 2002, **212**, 145-156.
19. M. Iqbal, *An introduction to solar radiation*, Elsevier, 1983.
20. J. Tian, Y. Sang, G. Yu, H. Jiang, X. Mu and H. Liu, *Advanced Materials*, 2013, **25**, 5075-5080.
21. Y. Tang, W. Di, X. Zhai, R. Yang and W. Qin, *ACS Catalysis*, 2013, **3**, 405-412.
22. G. Wang, B. Huang, X. Ma, Z. Wang, X. Qin, X. Zhang, Y. Dai and M. H. Whangbo, *Angewandte Chemie*, 2013, **125**, 4910-4913.
23. A. Gannoruwa, K. Niroshan, O. Ileperuma and J. Bandara, *Int. J. Hydrog. Energy*, 2014, 15411–15415.
24. M. A. M. Khan, S. Kumar, M. Ahamed, S. A. Alrokayan and M. S. AlSalhi, *Nanoscale research letters*, 2011, **6**, 1-8.
25. Y. Li, D.-S. Hwang, N. H. Lee and S.-J. Kim, *Chemical Physics Letters*, 2005, **404**, 25-29.
26. J. R. Beckett, D. Live, F.-D. Tsay, L. Grossman and E. Stolper, *Geochimica et Cosmochimica Acta*, 1988, **52**, 1479-1495.
27. J. R. Beckett, D. Live, F.-D. Tsay, L. Grossman and E. Stolper, *Geochimica et Cosmochimica Acta*, 1988, **52**, 1479-1495.
28. B. Erdem, R. A. Hunsicker, G. W. Simmons, E. D. Sudol, V. L. Dimonie and M. S. El-Aasser, *Langmuir*, 2001, **17**, 2664-2669.
29. H. Li, Z. Bian, J. Zhu, Y. Huo, H. Li and Y. Lu, *Journal of the American Chemical Society*, 2007, **129**, 4538-4539.
30. Y. Ohko, T. Tatsuma, T. Fujii, K. Naoi, C. Niwa, Y. Kubota and A. Fujishima, *Nat. Mater.*, 2002, **2**, 29-31.
31. G. B. Hoflund, Z. F. Hazos and G. N. Salaita, *Phys. Rev. B*, 2000, **62**, 11126.

32. L. Xu, B. Wei, W. Liu, H. Zhang, C. Su and J. Che, *Nanoscale research letters*, 2013, **8**, 1-7.
33. A. M. Ferraria, A. P. Carapeto and A. M. Botelho do Rego, *Vacuum*, 2012, **86**, 1988-1991.
34. W. Zhou, H. Liu, J. Wang, D. Liu, G. Du and J. Cui, *ACS applied materials & interfaces*, 2010, **2**, 2385-2392.
35. J. Yu, C. Trapalis, P. Zhang, G. Li and H. Yu, *Int. J. Photoenergy*, 2013, **2013**, 3.
36. J. Tominaga, *Journal of Physics: Condensed Matter*, 2003, **15**, R1101.
37. J. P. Allen, D. O. Scanlon and G. W. Watson, *Phys. Rev. B*, 2010, **81**, 161103.
38. I. Rabin, W. Schulze, G. Ertl, C. Felix, C. Sieber, W. Harbich and J. Buttet, *Chemical Physics Letters*, 2000, **320**, 59-64.
39. K. Naoi, Y. Ohko and T. Tatsuma, *Journal of the American Chemical Society*, 2004, **126**, 3664-3668.
40. R. Kötz and E. Yeager, *Journal of Electroanalytical Chemistry and Interfacial Electrochemistry*, 1980, **111**, 105-110.
41. D. Sarkar, C. K. Ghosh, S. Mukherjee and K. K. Chattopadhyay, *ACS Applied Materials and Interfaces*, 2013, **5**, 331-337.
42. Y. Tang, P. Wee, Y. Lai, X. Wang, D. Gong, P. D. Kanhere, T.-T. Lim, Z. Dong and Z. Chen, *The Journal of Physical Chemistry C*, 2012, **116**, 2772-2780.
43. T. Fukaya, D. Büchel, S. Shinbori, J. Tominaga, N. Atoda, D. P. Tsai and W. C. Lin, *Journal of Applied Physics*, 2001, **89**, 6139-6144.
44. A. V. Kolobov, A. Rogalev, F. Wilhelm, N. Jaouen, T. Shima and J. Tominaga, *Applied Physics Letters*, 2004, **84**, 1641-1643.
45. T. H. H. Le, K. Mawatari, Y. Pihosh, T. Kawazoe, T. Yatsui, M. Ohtsu, M. Tosa and T. Kitamori, *Applied Physics Letters*, 2011, **99**, 213105.
46. T. H. Le, K. Mawatari, K. Kitamura, T. Yatsui, T. Kawazoe, M. Ohtsu and T. Kitamori.
47. W. Weimer and M. Dyer, *Applied Physics Letters*, 2001, **79**, 3164-3166.
48. W. Ji-Fei, L. Hong-Jian, Z. Zi-You, L. Xue-Yong, L. Ju and Y. Hai-Yan, *Chinese Physics B*, 2010, **19**, 117310.
49. B. J. Morgan and G. W. Watson, *Physical Review B*, 2009, **80**, 233102.
50. L. Bertoluzzi, I. Herraiz-Cardona, R. Gottesman, A. Zaban and J. Bisquert, *The Journal of Physical Chemistry Letters*, 2014, **5**, 689-694.
51. S. Yukutake, T. Kawazoe, T. Yatsui, W. Nomura, K. Kitamura and M. Ohtsu, *Applied Physics B*, 2010, **99**, 415-422.
52. K. Tennakone and J. Bandara, *Solar energy materials and solar cells*, 2000, **60**, 361-365.
53. K. Onda, B. Li and H. Petek, *Physical Review B*, 2004, **70**, 045415.
54. M. Butler, M. Abramovich, F. Decker and J. Juliao, *Journal of The Electrochemical Society*, 1981, **128**, 200-204.
55. D. Pallotti, E. Orabona, S. Amoruso, C. Aruta, R. Bruzzese, F. Chiarella, S. Tuzi, P. Maddalena and S. Lettieri, *Journal of Applied Physics*, 2013, **114**, 043503.
56. L. Museur and A. Kanaev, *Journal of Applied Physics*, 2008, **103**, 103520-103520-103527.
57. S. Linic, P. Christopher and D. B. Ingram, *Nature materials*, 2011, **10**, 911-921.
58. A. Tanaka, K. Hashimoto, B. Ohtani and H. Kominami, *Chem. Commun.*, 2013, **49**, 3419-3421.
59. S. Merouani, O. Hamdaoui, Y. Rezgui and M. Guemini, *International Journal of Hydrogen Energy*, 2015, DOI: 10.1016/j.ijhydene.2015.01.150.
60. L. Gomathi Devi and K. Mohan Reddy, *Applied Surface Science*, 2011, **257**, 6821-6828.
61. X. Wang, S. Li, H. Yu, J. Yu and S. Liu, *Chemistry-a European Journal*, 2011, **17**, 7777-7780.
62. R. N. Noufi, P. A. Kohl, S. N. Frank and A. J. Bard, *Journal of The Electrochemical Society*, 1978, **125**, 246-252.
63. C. Zhao, A. Krall, H. Zhao, Q. Zhang and Y. Li, *International Journal of Hydrogen Energy*, 2012, **37**, 9967-9976.

TOC

IR photon initiated photocatalytic hydrogen production of the catalyst Ag_2O/TiO_2 is demonstrated and the functions of Ag_2O and TiO_2 in "dark photocatalysis" are discussed.